Optimal Motion Generation for Groups of Robots: A Geometric Approach

Calin Belta
MEM Department,
Drexel University,
Philadelphia, PA 19104
e-mail: calin@drexel.edu

Vijay Kumar
GRASP Laboratory,
University of Pennsylvania,
Philadelphia, PA 19104
e-mail: kumar@grasp.cis.upenn.edu

In this paper we generate optimal smooth trajectories for a set of fully-actuated mobile robots. Given two end configurations, by tuning one parameter, the user can choose an interpolating trajectory from a continuum of curves varying from that corresponding to maintaining a rigid formation to motion of the robots toward each other. The idea behind our method is to change the original constant kinetic energy metric in the configuration space and can be summarized into three steps. First, the energy of the motion as a rigid structure is decoupled from the energy of motion along directions that violate the rigid constraints. Second, the metric is "shaped" by assigning different weights to each term. Third, geodesic flow is constructed for the modified metric. The optimal motions generated on the manifolds of rigid body displacements in 3-D space $(SE(3))$ or in plane $(SE(2))$ and the uniform rectilinear motion of each robot corresponding to a totally uncorrelated approach are particular cases of our general treatment.
[DOI: 10.1115/1.1641190]

1 Introduction

Multi-robot systems have applications in exploration missions, military surveillance, and cooperative manipulation tasks. Recent research on such systems include work on multi-robot motion planning [1], cooperative manipulation [2], mapping and exploration [3], behavior-based formation control [4], and software architectures for multi-robotic systems [5]. In all these paradigms, one is interested in planning the motion for a team of robots, and in many cases it is important for the robots to maintain a formation. In multi-robot manipulation, for example, it is necessary for the robots to maintain constraints on the relative position and orientation to guarantee form, force, or object closure [6]. In multi-robot mapping or target tracking, it is essential for the robots to maintain an optimal formation to minimize the errors associated with the estimation process [7]. Finally, it is well known that formation flying results in great benefits in terms of fuel efficiency [8]. In addition, there are also strategic benefits to be derived from maintaining formation in military operations in air, ground, or water [9].

In this paper, we first consider the formation of robots as a rigid body, and investigate the motion of such a formation. Virtual structures [10] have been used for motion planning, coordination and control of space-crafts [11]. Our definition of a rigid formation requires that distances between chosen reference points on robots remain fixed. The relative orientations of each robot are not restricted in such a formulation. To this end, we build on the results from [12] to generate trajectories that satisfy the rigidity constraint and minimize the overall energy. The optimization problem is reduced to generating geodesics on the Lie groups $SO(3)$ and $SE(3)$. Due to the geometrical framework that we use, the generated trajectories are left invariant i.e., independent of the choice of the inertial frame $\{F\}$.

However, the rigid formation constraint is too restrictive in many applications. We would like the robots to be able to break formation, cluster together or string themselves out to avoid obstacles, and to regroup to achieve a desired goal formation at the destination. We next develop a family of trajectories ranging from the ones that are optimal for a rigid formation on one hand to independent trajectories that are optimal for each robot on the other. This is done by constructing a new metric which is obtained from the naturally induced (constant) kinetic energy metric derived from the inertial properties of the robots. The tangent space at each point of the configuration space is decomposed into two metric-orthogonal subspaces. We then assign different weights to the terms corresponding to rigid and nonrigid instantaneous motions to derive a new "shaped" metric. This idea of a "decomposition" and a subsequent "modification" is closely related to the methodology of controlled Lagrangians described in [13,14]. Optimal curves derived from this metric yield the planned trajectories for individual robots.

The rest of the paper is organized as follows. We state the main problem and introduce the notation in Section 2. A brief overview of the geometry of rigid body motion is given in Section 3. Section 4 gives a mathematical description of the constraint that a set of points in 3D are rigidly connected, in terms of a smoothly varying distribution in the configuration space. This distribution and its orthogonal complement in the kinetic energy metric are used to separate rigid and non-rigid motions in Section 5 and to define "shaped" metrics in Section 7. Section 6 is concerned with optimal motion plans for virtual structures while Section 7 shows how continua of trajectories can be constructed by using metric shaping. The paper concludes with final remarks and outline of future work in Section 8.

2 Problem Statement and Notation

Consider N robots moving (rotating and translating) in 3-D space with respect to an inertial frame $\{F\}$. We choose a reference point on each robot at its center of mass O_i. A moving frame $\{M_i\}$ is attached to each robot at O_i (see Fig. 1).

Robot i has mass m_i and matrix of inertia H_i with respect to frame $\{M_i\}$. Let $R_i \in SO(3)$ denote the rotation of $\{M_i\}$ in F and $q_i \in \mathrm{IR}^3$ the position vector of O_i in $\{F\}$. Let ω_i denote the expression in $\{M_i\}$ of the angular velocity of $\{M_i\}$ with respect to $\{F\}$. The *formation* is defined by the reference points O_i. The moving formation is called rigid if the relative distance between any of the points O_i is maintained constant. Sometimes it is also useful to define a formation frame $\{M\}$, attached at some virtual point O' and with pose $(R,d) \in SE(3)$ in $\{F\}$. Let q_i^0 denote the position vectors of O_i in $\{M\}$.

The configuration space is the $6N$-dimensional manifold, $SE(3) \times SE(3) \times \ldots SE(3)$, given by the poses of each robot.

Contributed by the Mechanisms and Robotics Committee for publication in the JOURNAL OF MECHANICAL DESIGN. Manuscript received August 2002; revised June 2003. Associate Editor: M. Raghavan.

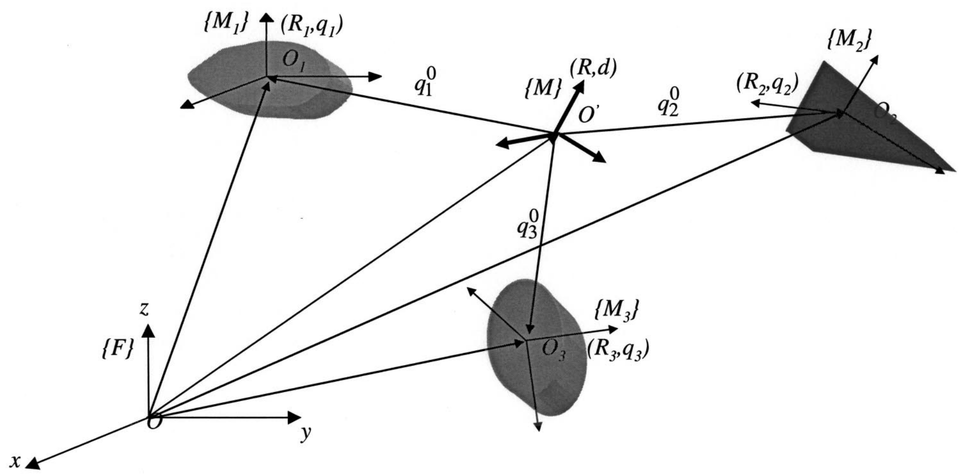

Fig. 1 A set of $N=3$ robots

Given two configurations at times $t=0$ and $t=1$ respectively, the goal is to generate smooth interpolating motion for each robot so that the total kinetic energy is minimized.

The kinetic energy T of the system of robots is the sum of the individual energies. Since the frames $\{M_i\}$ are placed at the centroids O_i of the robots, T can be written as the sum of the total rotational energy T_r and the total translational energy T_t in the form:

$$T=T_r+T_t, \quad T_r=\frac{1}{2}\sum_{i=1}^{N}(\omega_i^T H_i \omega_i), \quad T_t=\frac{1}{2}\sum_{i=1}^{N}(m_i \dot{q}_i^T \dot{q}_i) \tag{1}$$

Since our definition of a formation only involves the reference points O_i, a formation requirement will only constrain the q_i's from the above equation. Therefore, due to the decomposition in Eq. (1), minimizing the total energy is equivalent to solving $N+1$ independent optimization subproblems:

$$\min_{\sigma_i}\int_0^1 \omega_i^T H_i \omega_i dt, \quad i=1,\ldots,N, \tag{2}$$

$$\min_{q_i=1,\ldots,N}\int_0^1 T_t dt \tag{3}$$

where σ_i is some parameterization of the rotation of $\{M_i\}$ in $\{F\}$, i.e., some local coordinates on $SO(3)$. The solutions to Eqs. (2) are given by N geodesics on $SO(3)$ with left invariant metrics with matrices H_i. Two different methods to obtain the solution are given in [12,15] and a short example is given in Section 6.

The main focus in this paper is solving problem (3) while satisfying constraints on the positions of the reference points O_i that may be imposed by the requirements on the task. Thus the configuration space we are interested in is just the $3N$ dimensional $Q=\{q|q=(q_1,\ldots,q_N)\}$, which collects all the position vectors of the chosen reference points. Maintaining a rigid formation (a virtual structure) imposes constraints on the configuration space, Q, and these constraints may be relaxed as necessary.

3 Background

In this section we give a brief overview of the geometry of rigid body motion, mainly to introduce the notation. The special Euclidean group $SE(3)$ is the set of all rigid displacements in IR^3:

$$SE(3)=\left\{g \middle| g=\begin{bmatrix} R & d \\ 0 & 1\end{bmatrix}, R\in \mathrm{IR}^{3\times 3}, RR^T=I, \det R=1, d\in \mathrm{IR}^3\right\}.$$

The Lie algebra of $SE(3)$, denoted by $se(3)$, is given by:

$$se(3)=\left\{\hat{s}\middle|\hat{s}=\begin{bmatrix}\hat{\omega} & v \\ 0 & 0\end{bmatrix}, \hat{\omega}\in \mathrm{IR}^{3\times 3}, \hat{\omega}^T=-\hat{\omega}, v\in \mathrm{IR}^3\right\}$$

where $\hat{\omega}$ is the skew-symmetric matrix form of the vector $\omega \in \mathrm{IR}^3$ and $s=(\omega,v)\in \mathrm{IR}^6$. Given a curve $g(t)=(R(t),d(t))$, an element $s(t)$ of the Lie algebra $se(3)$ can be associated to the tangent vector $\dot{g}(t)$ by:

$$\hat{s}(t)=g^{-1}(t)\dot{g}(t)=\begin{bmatrix}\hat{\omega}(t) & R^T\dot{d} \\ 0 & 0\end{bmatrix} \tag{4}$$

where $\hat{\omega}(t)=R^T\dot{R}$.

Consider a rigid body moving in free space. Assume any inertial reference frame $\{F\}$ fixed in space and a frame $\{M\}$ fixed to the body at point O'. A curve on $SE(3)$ physically represents a motion of the rigid body. If $\{\omega(t),v(t)\}$ is the vector pair corresponding to $s(t)$, then ω corresponds to the angular velocity of the rigid body while v is the linear velocity of O', both expressed in the frame $\{M\}$.

For any $s_1,s_2\in se(3)$ and G a positive definite matrix, we can define a metric $s_1^T G s_2$ on the Lie algebra $se(3)$ and extend it through left translation throughout the manifold $SE(3)$. Let m be the mass of a rigid body and H its matrix of inertia with respect to a body frame $\{M\}$, assumed at the center of mass. Then, with

$$G=\frac{1}{2}\begin{bmatrix} H & 0 \\ 0 & mI_3\end{bmatrix} \tag{5}$$

the norm induced by the above metric $s^T G s$ is exactly the kinetic energy of the moving (rotating and translating) rigid body. Moreover, if $\{M\}$ is aligned with the principal axes, then H is diagonal.

For a rigid system of N particles with masses $m_1,\ldots,m_N$ and position vectors $q_1^0,\ldots,q_N^0$ in the body fixed frame $\{M\}$, the matrix of the (left invariant) kinetic energy metric on $SE(3)$ is [16]:

$$M=\begin{bmatrix} -\sum_{i=1}^{N} m_i \hat{q}_i^{0^2} & \sum_{i=1}^{N} m_i \hat{q}_i^0 \\ -\sum_{i=1}^{N} m_i \hat{q}_i^0 & \sum_{i=1}^{N} m_i I_3\end{bmatrix} \tag{6}$$

The upper left 3×3 sub-matrix of M is the inertia matrix of the system of particles with respect to $\{M\}$. If frame $\{M\}$ is placed at the center of mass and aligned with the principal axes of the structure, then M becomes diagonal.

The geodesics on a differentiable manifold can be defined as minimum length, or equivalently, minimum energy curves [17]. A useful (local) characterization of a geodesic curve on a n-dimensional Riemannian manifold (locally) parameterized by $x_1, \ldots, x_n$ is the following set of differential equations:

$$\ddot{x}_i + \sum_{j,k} \Gamma^i_{jk} \dot{x}_j \dot{x}_k = 0, \quad i = 1, \ldots, n \tag{7}$$

where Γ^i_{jk} are the Christoffel symbols of the unique symmetric connection associated to the metric on the manifold [17].

In [12] it has been proved that a geodesic $g(t)$ on $SE(3)$ equipped with a left invariant product metric of the type (5) is composed of the geodesics in the component manifolds $SO(3)$ and IR^3 with the corresponding component metrics, and are described by the following set of differential equations:

$$\frac{d\omega}{dt} = -H^{-1}(\omega \times (H\omega)) \tag{8}$$

$$\ddot{d} = 0. \tag{9}$$

If $H = \alpha I$, an analytical expression for the geodesic passing through $g(0) = (R(0), d(0))$ and $g(1) = (R(1), d(1))$ at $t = 0$ and $t = 1$ respectively, is given by [18] $g(t) = (R(t), d(t))$, where $R(t) = R(0)\exp(\hat{\omega}_0 t)$, $d(t) = (d(1) - d(0))t + d(0)$ and $\hat{\omega}_0 = \log(R(0)^T R(1))$. In the case when $H \neq \alpha I$, there is no closed form expression for the corresponding geodesic and numerical methods or the projection method [15,19] should be employed.

4 The Rigidity Constraint

The group of N robots is said to form a *virtual structure* if the relative distance between any of the reference points O_i is maintained constant. Let $q = [q_1^T, \ldots, q_N^T]^T$ denote an arbitrary point in Q. For an arbitrary pair of reference points with position vectors q_i and q_j, $i, j = 1, \ldots, N$, $i < j$, the constraints can be written as:

$$(q_i - q_j)^T (q_i - q_j) = constant \tag{10}$$

or, by differentiation:

$$(q_i - q_j)^T \dot{q}_i - (q_i - q_j)^T \dot{q}_j = 0$$

By lifting this constraint to the configuration manifold Q, the coordinates of the corresponding differential one form can be written as a $1 \times 3N$ row vector:

$$\omega_{ij} = [0 \quad \ldots \quad 0 (q_i - q_j)^T \quad 0 \quad \ldots \quad 0 - (q_i - q_j)^T \quad 0 \quad \ldots \quad 0]$$

The non-zero 1×3 blocks in the above matrix are in positions i and j, respectively. If we consider all $(N-1)N/2$ possible constraints, we can construct the codistribution ω_R as the span of all the corresponding covectors:

$$\omega_R = \mathrm{span}\{\omega_{ij}, i, j = 1, \ldots, N, i < j\}$$

It is obvious that not all the $(N-1)N/2$ covectors (constraints) are independent. To insure rigidity, it is necessary and sufficient to impose $2N-3$ constraints of the type (10) in plane, while in 3D, the number is $3N-6$. By simple inspection, it is easy to prove that the annihilating distribution of ω_R ($\omega_R(\Delta_R) = 0$) is:

$$\Delta_R = \mathrm{Range}(A(q)), \quad A(q) = \begin{bmatrix} -\hat{q}_1 & I_3 \\ \ldots & \ldots \\ -\hat{q}_N & I_3 \end{bmatrix} \tag{11}$$

Therefore, by lifting each constraint to the configuration manifold Q, the virtual structure (rigidity) constraint can be written as

$$\dot{q} \in \Delta_R(q) \tag{12}$$

If q_i are not all contained in any proper hyperplane of IR^d ($d = 2,3$), it can be proved [20] that the distribution Δ_R is regular, and, therefore integrable, since involutivity is always guaranteed. The distribution $\Delta_R(q)$ determines a foliation of Q with leaves given by orbits of $SE(3)$. Indeed, assume $q(0) = q^0$ and $\dot{q}(0) \in \Delta_R(q^0)$. Then, the rigidity constraint (12) is satisfied for all $t \geqslant 0$ if and only if

$$q_i(t) = d(t) + R(t) q_i^0, \quad i = 1, \ldots, N \tag{13}$$

where $(R(t), d(t))$ is a trajectory of the left invariant control system

$$\dot{g}(t) = g\hat{s} \tag{14}$$

starting from $R(0) = I_3$, $d(0) = 0$.

Note that, under the rigidity assumption (12), the coordinates r of the expansion of $\dot{q} \in \Delta_R(q)$ along the columns of $A(q)$, i.e., $\dot{q} = A(q)r$, are exactly the components of the left invariant twist of a virtual structure formed by $(q_1, \ldots, q_N)$ and $\{F\}$ at that instant.

Also, if (12) is satisfied, then s from (14) is the left invariant twist of a moving rigid structure formed by $(q_1^0, \ldots, q_N^0)$ and $\{M\}$ and for which the mobile frame $\{M\}$ was coincident with $\{F\}$ at $t = 0$. $g = (R, d)$ is the pose of the moving frame $\{M\}$ in $\{F\}$. Moreover, we have

$$\dot{q}_i = R[-\hat{q}_i^0 I]s \tag{15}$$

It follows that motion planning (control) problems for a set of N robots in 3D required to maintain a rigid formation can be reduced to motion planning (control) problems for a left invariant control system on $SE(3)$.

5 Motion Decomposition: Rigid vs. Nonrigid

We first define a metric $\langle , \rangle$ in the position configuration space, which is the same at all points $q \in Q$:

$$\langle V_q^1, V_q^2 \rangle = V_q^{1\,T} M V_q^2, \tag{16}$$

$$V_q = \dot{q} \in T_q Q, \quad M = \frac{1}{2} \mathrm{diag}\{m_1 I_3, \ldots, m_N I_3\}$$

Metric (16) is called the *kinetic energy metric* because its induced norm ($V_q^1 = V_q^2 = \dot{q}$) assumes the familiar expression of the kinetic energy of the system $1/2 \Sigma_{i=1}^N m_i \dot{q}_i^T \dot{q}_i$.

If no restrictions are imposed on Q, the geodesic between $q(0) = q^0$ and $q(1) = q^1$ for metric (16) is obviously a straight line uniformly parameterized in time interpolating between q^0 and q^1 in Q.

At each point q in the configuration space Q, $\Delta_R(q)$ locally describes the set of all rigid body motion directions. The orthogonal complement to $\Delta_R(q)$, $\Delta_{NR}(q)$ will be the set of all directions violating the rigid body constraints.[1] For an arbitrary tangent vector $V_q \in T_q Q$, let $\mathbf{R}V_q$ denote the projection onto Δ_R and $\mathbf{NR}V_q$ denote the projection onto Δ_{NR}.

Using metric (16), the orthogonal complement of the "rigid" distribution $\Delta_R(q)$ is the "nonrigid" distribution

$$\Delta_{NR}(q) = \mathrm{Null}(A(q)^T M) \tag{17}$$

Let $B(q)$ denote a matrix whose columns are a basis of $\Delta_{NR}(q)$.

Let ψ denote the components of the projection in this basis: $\mathbf{NR}V_q = B(q)\psi$. Therefore, the velocity at point q can be written as:

$$V_q = \mathbf{R}V_q + \mathbf{NR}V_q = A(q)r + B(q)\psi \tag{18}$$

Then, for any $V_q^1, V_q^2 \in T_q Q$, we have:

[1] In [13,14], the tangent space at q to the orbit of $SE(3)$ is called the vertical space at q, Ver_q, and its orthogonal complement is the horizontal space at $q \in Q$, Hor_q.

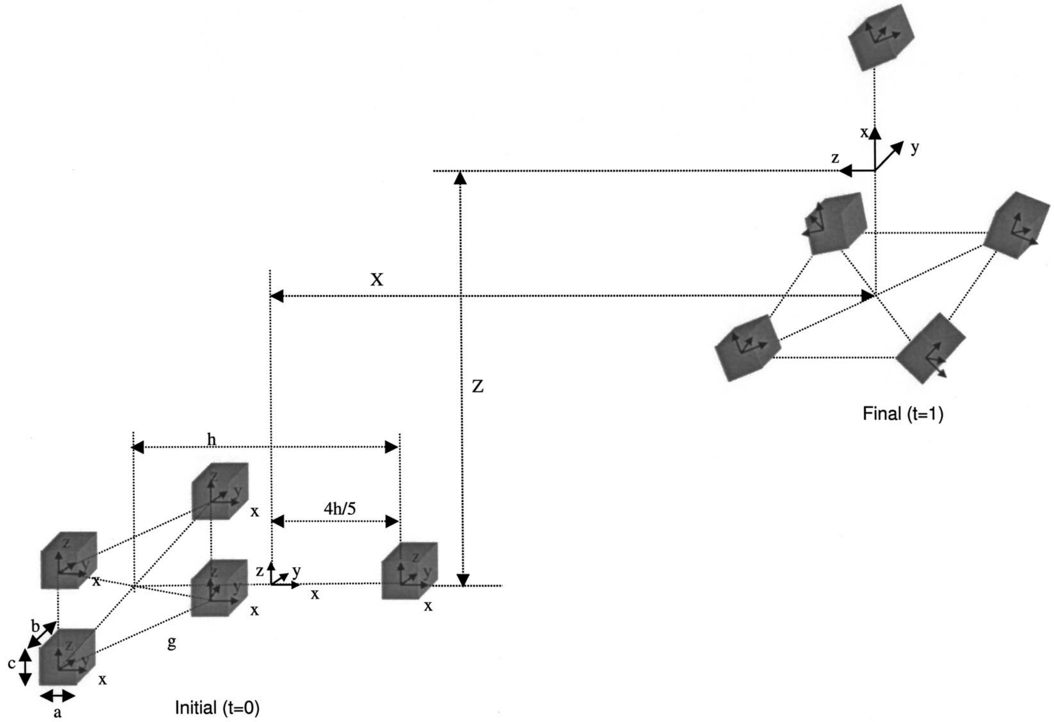

Fig. 2 Geometry of the robots and of the virtual structure showing the initial and the final configurations. The relevant dimensions are chosen to be: $a=c=2$, $b=10$, $h=20$, $l=10$, $X=20$, $Z=20$, $m=12$.

$$
\begin{aligned}
\langle V_q^1, V_q^2\rangle &= V_q^{1^T} M V_q^2 = r^{1^T} A^T M A r^2 + r^{1^T} A^T M B \psi^2 + \psi^{1^T} B^T M A r^2 \\
&\quad + \psi^{1^T} B^T M B \psi^2 = r^{1^T} A^T M A r^2 + \psi^{1^T} B^T M B \psi^2 \\
&= \langle B\psi^1, B\psi^2\rangle + \langle Ar^1, Ar^2\rangle = \langle \mathbf{NR} V_q^1, \mathbf{NR} V_q^2\rangle \\
&\quad + \langle \mathbf{R} V_q^1, \mathbf{R} V_q^2\rangle
\end{aligned}
$$

because both $A^T M B$ and $B^T M A$ are zero from (17). Also, note that

$$
\begin{aligned}
r &= (A^T M A)^{-1} A^T M V, \\
\psi &= (B^T M B)^{-1} B^T M V
\end{aligned} \tag{19}
$$

where the explicit dependence of A and B on q was omitted for simplicity. Therefore, the translational kinetic energy (which is the square of the norm induced by metric (16) becomes:

$$
T_t(q,\dot{q}) = \dot{q}^T M \dot{q} = r^T A^T M A r + \psi^T B^T M B \psi \tag{20}
$$

In (20), $r^T A^T M A r$ captures the energy of the motion of the system of particles as a rigid body, while the remaining part $\psi^T B^T M B \psi$ is the energy of the motion that violates the rigid body restrictions. For example, in the obvious case of a system of $N=2$ particles, the first part corresponds to the motion of the two particles connected by a rigid massless rod, while the second part would correspond to motion along the line connecting the two bodies.

6 Motion Generation for Rigid Formations

In this section, we will assume that the robots are required to move in rigid formation, i.e., the distances between any two reference points O_i are preserved, or, equivalently, the reference points form a rigid polyhedron.

In our geometric framework, the rigid body requirement means restricting the trajectory $q(t) \in Q$ to be a $SE(3)$-orbit, or equivalently, $\mathbf{NR}\dot{q}=0$ or $\dot{q} \in \Delta_R(q)$, for all q.

In this case, one can imagine a body frame $\{M\}$ moving with the virtual structure determined by the O_i's. Initially $(t=0)$, the frame $\{M\}$ is coincident with $\{F\}$ and $q(0)=q^0$. The position vector of O_i in $\{M\}$ is constant during this motion and equal to q_i^0.

From (15) and (1), the kinetic energy T_t becomes:

$$
T_t = s^T \mathcal{M} s, \quad \mathcal{M} = A(q^0)^T M A(q^0) \tag{21}
$$

where $s \in se(3)$ is the instantaneous twist of the virtual structure and A is given by (11). The expression of $\mathcal{M}$ in (21) can be easily seen to coincide with (6).

Therefore, if the set of robots is required to move while maintaining a constant shape q^0, the optimization problem is reduced from dimension $6N$ to dimension $3N+6$, and consists of solving for N geodesics on $SO(3)$ with metrics H_i (individual rotations) and one geodesic on the $SE(3)$ of the virtual structure with left invariant metric $\mathcal{M}$ as in (21). If $\mathcal{M}$ has a product structure as in (5), then the translational part of the geodesic on $SE(3)$ is easily solvable leading to a polynomial curve. To construct interpolating geodesics on $SO(3)$, a numerical method such as relaxation or shooting [21] can be used to solve the corresponding boundary value problem. In this case, one needs to choose a parameterization of $SO(3)$ and three more differential equations in these local coordinates will augment system (8). An alternative is to use the projection method described in [15,19]. The resulting computation is less expensive but the trajectories are sub-optimal.

For illustration, we consider five identical parallelepipedic robots $m_i=m, i=1,\ldots,5$ required to move in formation while minimizing energy. The initial and final poses together with the geometrical properties of the robots are given in Fig. 2. The body frames and the formation frame placed at the center of mass and aligned with the principal axis are drawn. The inertial frame is coincident with the formation frame at $t=0$. As seen from the inertial frame, the formation frame is translated by $(X,0,Z)$ and rotated by -90 degrees around the y-axis.

As outlined in the previous section, generating optimal motion for this group of robots reduces to generating five geodesics on the $SO(3)$ of each robot with left invariant metric

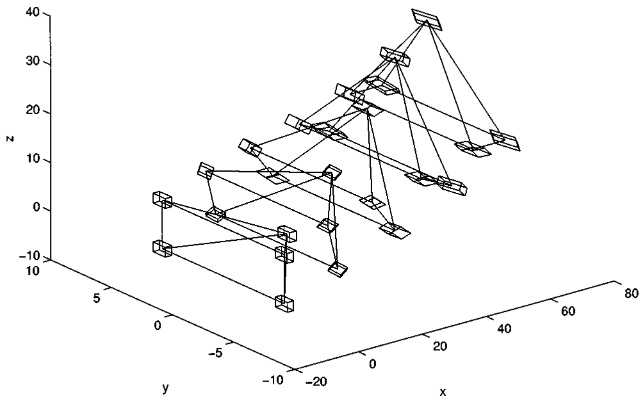

Fig. 3 Optimal motion for five identical robots required to maintain a rigid formation

$$H_i=\frac{m}{24}\begin{bmatrix} b^2+c^2 & 0 & 0 \\ 0 & a^2+c^2 & 0 \\ 0 & 0 & a^2+b^2 \end{bmatrix}, \quad i=1,\ldots,5$$

and one geodesic on the $SE(3)$ of the virtual structure endowed with a left invariant metric with matrix

$$G=\frac{m}{2}\begin{bmatrix} 2l^2 & 0 & 0 & 0 \\ 0 & l^2+\frac{4h^2}{3} & 0 & 0 \\ 0 & 0 & l^2+\frac{4h^2}{3} & 0 \\ 0 & 0 & 0 & 3I_3 \end{bmatrix}$$

We used the relaxation method to solve the corresponding boundary value problem. Exponential coordinates were employed as local parameterization of $SO(3)$ [19]. The resulting motion is presented in Fig. 3.

7 Motion Generation by Kinetic Energy Shaping

By shaping the kinetic energy, we mean smoothly changing the corresponding metric (16) at T_qQ so that motion along some specific directions is allowed while motion along some other directions is penalized. The new metric will no longer be constant-the Christoffel symbols of the corresponding symmetric connection will be non-zero. The associated geodesic flow gives optimal motion.

In this work, the original metric (16) is shaped by putting different weights on the terms corresponding to the rigid and non-rigid motions:

$$\langle V_q^1, V_q^2\rangle_\alpha=\alpha\langle \mathbf{NR}V_q^1, \mathbf{NR}V_q^2\rangle+(1-\alpha)\langle \mathbf{R}V_q^1, \mathbf{R}V_q^2\rangle \tag{22}$$

Using (19) to go back to the original coordinates, we get the modified metric in the form:

$$\langle V_q^1, V_q^2\rangle_\alpha=V_q^{1^T} M_\alpha(q) V_q^2, \tag{23}$$

where the new matrix of the metric is now dependent on the artificially introduced parameter α and the point on the manifold $q\in Q$:

$$M_\alpha(q)=\alpha MA(A^TMA)^{-T}A^TM+(1-\alpha)MB(B^TMB)^{-T}B^TM \tag{24}$$

The significance of the shaping parameter α can be best understood by examining metric (22) when α increases from 0 to 1. First, note that for $\alpha=0$ and $\alpha=1$ matrix (24) of metric (22) becomes singular and cannot be used to construct geodesic flow. Indeed, since M is nonsingular, the rank of the first term of the sum in (24) is equal to the rank of A, which is 6 if q_i are not all contained in a hyperplane, while the rank of the second term in the sum is equal to the rank of B, which is $3N-6$. Making $\alpha=0$ is equivalent to completely forbiding motions along orbits of $SE(3)$. For example, for two bodies, they are only allowed to move along the line connecting them. When α is slightly larger than zero, matrix (24) of metric (22) becomes non-singular and motion can be generated between arbitrary initial and final positions. However, the motion along the rigid directions contained in the distribution Δ_R are penalized. "Most" of the motion will be along the non-rigid directions. The corresponding geodesics of metric (24) will cause the robots to cluster together through most of the duration of the trajectory. As α approaches 0.5, the Christoffel symbols become zero and the weights given to the rigid and nonrigid terms in metric (24) are equal. This case corresponds to optimal uncoordinated interpolating motions of the individual robots, i.e., straight lines uniformly parameterized in time. As α tends to 1, the non-rigid motion along the directions contained in the distribution Δ_{NR} is penalized. What is left is "mostly rigid" motion, and the corresponding geodesics represent almost *optimal rigid motion*. $\alpha=1$ is equivalent to completely forbiding non-rigid motions.

We use the geodesic flow of metric (23) to produce smooth interpolating motion between two given configurations:

$$q^0=q(0), \quad q^1=q(1)\in \mathrm{IR}^{3N} \tag{25}$$

To simplify the notation, let x_i, $i=1,\ldots,3N$ denote the coordinates $q_i\in\mathrm{IR}^3$, $i=1,\ldots,N$ on the configuration manifold Q. In these coordinates, the geodesic flow is described by differential Eqs. (7) with $n=3N$ and Γ_{ij}^k are the Christoffel symbols of the unique symmetric connection associated to metric (23):

$$\Gamma_{ij}^k=\frac{1}{2}\sum_h\left(\frac{\partial m_{hj}}{\partial x^i}+\frac{\partial m_{ih}}{\partial x^j}-\frac{\partial m_{ij}}{\partial x^h}\right)m^{hk} \tag{26}$$

m_{ij} and m^{ij} are elements of M_α and M_α^{-1}, respectively.

Because $\alpha=0$ and $\alpha=1$ make the metric singular, (2) can only be used for $0<\alpha<1$.

7.1. Two Bodies in Plane. Consider two bodies of masses m_1 and m_2 moving in the $x-y$ plane. The configuration space is $Q=R^4$ with coordinates $q=[x_1, y_1, x_2, y_2]^T$. The A and B matrices describing $\Delta_R(q)$ and $\Delta_{NR}(q)$ as in (11) and (17) are:

$$A=\begin{bmatrix} -y_1 & 1 & 0 \\ x_1 & 0 & 1 \\ -y_2 & 1 & 0 \\ x_2 & 0 & 1 \end{bmatrix}, \quad B=\begin{bmatrix} \frac{m_2(x_2-x_1)}{m_1(y_1-y_2)} \\ -\frac{m_2}{m_1} \\ \frac{x_1-x_2}{y_1-y_2} \\ 1 \end{bmatrix} \tag{27}$$

From (27), (24), and (26), after some trivial but rather tedious calculations, we get the 64 Christoffel symbols $\Gamma^k=(\Gamma_{ij}^k)_{ij}$ of the connection associated with the modified metric at $q\in Q$ in the form:

$$\Gamma^1=\frac{2(1-2\alpha)}{\alpha}\frac{m_2}{m_1+m_2}\frac{d_x}{(d_x^2+d_y^2)^2}\Gamma$$

$$\Gamma^2=\frac{2(1-2\alpha)}{\alpha}\frac{m_2}{m_1+m_2}\frac{d_y}{(d_x^2+d_y^2)^2}\Gamma$$

$$\Gamma^3=-\frac{2(1-2\alpha)}{\alpha}\frac{m_1}{m_1+m_2}\frac{d_x}{(d_x^2+d_y^2)^2}\Gamma$$

$$\Gamma^4=-\frac{2(1-2\alpha)}{\alpha}\frac{m_1}{m_1+m_2}\frac{d_y}{(d_x^2+d_y^2)^2}\Gamma$$

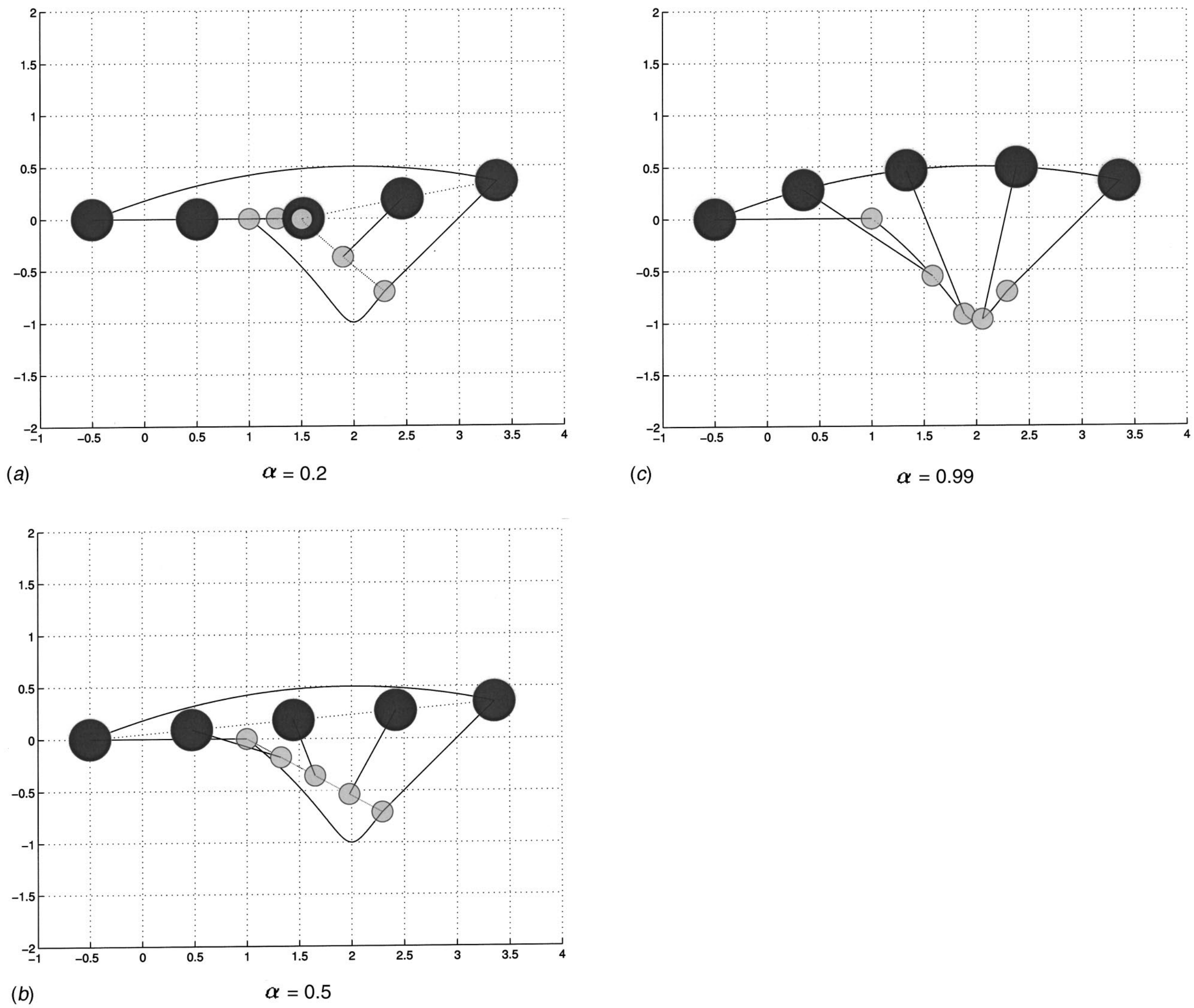

Fig. 4 Three interpolating motions for a set of two planar robots as geodesics of a modified metric defined in the configuration space.

where

$$\Gamma = \begin{bmatrix} -d_y^2 & d_x d_y & d_y^2 & -d_x d_y \\ d_x d_y & -d_x^2 & -d_x d_y & d_x^2 \\ d_y^2 & -d_x d_y & -d_y^2 & d_x d_y \\ -d_x d_y & d_x^2 & d_x d_y & -d_x^2 \end{bmatrix}$$

and $d_x = x_1 - x_2$, $dy = y_1 - y_2$. It can be easily seen that, as expected, all Christoffel symbols are zero if $\alpha = 0.5$. Also, the actual masses of the robots are not relevant, it's only the ratio m_1/m_2 which is important.

In this example, we assume $m_2 = 2m_1$ and the boundary conditions:

$$q^0 = \begin{bmatrix} 1 \\ 0 \\ -0.5 \\ 0 \end{bmatrix}, \quad q^1 = \begin{bmatrix} 3 - \frac{\sqrt{2}}{2} \\ -\frac{\sqrt{2}}{2} \\ 3 + \frac{\sqrt{2}}{4} \\ \frac{\sqrt{2}}{4} \end{bmatrix}$$

which correspond to a rigid body displacement so that we can compare our results to the optimal motion corresponding to a rigid body.

If the structure was assumed rigid, then the optimal motion is described by uniform rectilinear translation of the center of mass between (0,0) and (3,0) and uniform rotation between 0 and $3\pi/4$ around $-z$ placed at the center of mass. The corresponding trajectories of the robots are drawn in solid line in all the pictures in Fig. 4. It can be easily seen that there is no difference between the optimal motion of the virtual structure solved on $SE(2)$ and the geodesic flow of the modified metric with $\alpha = 0.99$ (Fig. 4, bottom). If $\alpha = 0.5$, all bodies move in straight line as expected (Fig. 4, middle). For $\alpha = 0.2$, the bodies go toward each other first, and then split apart to attain the final positions (Figure 4, top).

7.2. Three Bodies in Plane. The calculation of the trajectories for three bodies moving in the plane is simplified by assuming that the robots are identical, and, without loss of generality, we assume $m_1 = m_2 = m_3 = 1$. The rigid and the non-rigid spaces at a generic configuration

$$q = [x_1, y_1, x_2, y_2, x_3, y_3]^T \in Q = \mathrm{IR}^6$$

are given by

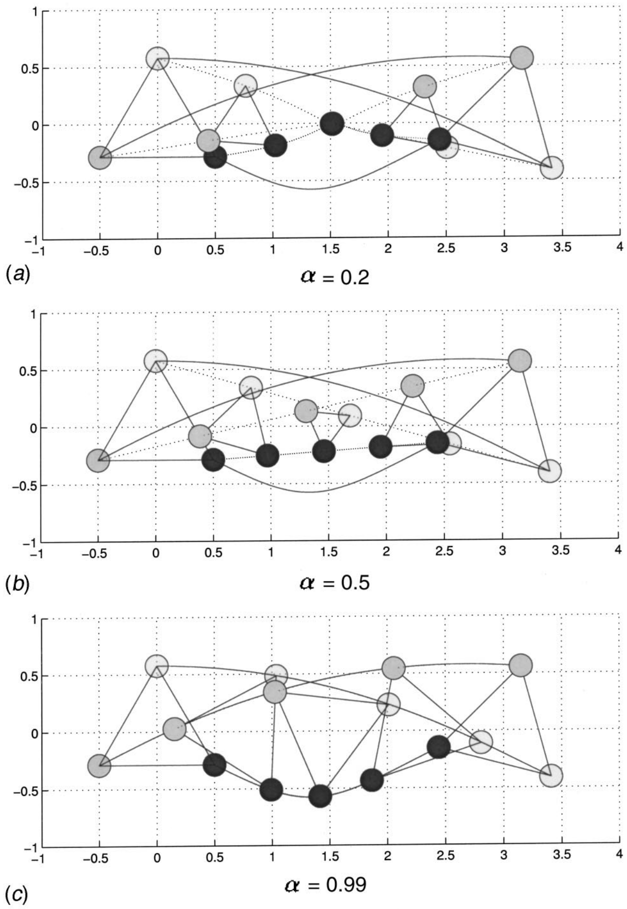

Fig. 5 Three interpolating motions for a set of three planar robots as geodesics of a modified metric defined in the configuration space.

$$\Delta_R = \text{Range}(A), \quad A = \begin{bmatrix} -y_1 & 1 & 0 \\ x_1 & 0 & 1 \\ -y_2 & 1 & 0 \\ x_2 & 0 & 1 \\ -y_3 & 1 & 0 \\ x_3 & 0 & 1 \end{bmatrix},$$

$$\Delta_{NR} = \text{Range}(B), \quad B = \begin{bmatrix} \frac{x_3 - x_1}{y_1 - y_2} & \frac{y_2 - y_3}{y_1 - y_2} & \frac{x_2 - x_1}{y_1 - y_2} \\ -1 & 0 & -1 \\ \frac{x_1 - x_3}{y_1 - y_2} & \frac{y_3 - y_1}{y_1 - y_2} & \frac{x_1 - x_2}{y_1 - y_2} \\ 0 & 0 & 1 \\ 0 & 1 & 0 \\ 1 & 0 & 0 \end{bmatrix}$$

For simplicity, we omit the expressions of the modified metric and of the Christoffel symbols, which are rather involved. The simulation scenario resembles the one in Section 7.1: the end poses correspond to a rigid structure consisting of a equilateral triangle with side equal to 1. The optimal trajectory solved on $SE(2)$ corresponds to rectilinear uniform motion of the center of mass (line between (0,0) and (3,0) in Fig. 5) and uniform rotation from angle 0 to $3\pi/4$ around axis $-z$. The resulting motion of each robot is shown solid, while the actual trajectory for the corresponding value of α is shown dashed. First note for $\alpha = 0.99$ the trajectories are basically identical with the optimal traces produced by the virtual structure, as expected. In the case $\alpha = 0.5$ the bodies move in straight line (corresponding to the unmodified metric). The tendency to cluster as α decreases is seen for $\alpha = 0.2$. Note also that due to our choice $m_1 = m_2 = m_3$, the geometry of the equilateral triangle is preserved for all values of α, it only scales down when α decreases from 1.

In both Sections 7.1 and 7.2, the motions were produced using the boundary value problem solver "bvp4c" from MATLAB, which is based on a relaxation type procedure [21]. Since the differential equations of the geodesics (7) are of second order in each coordinate, the state space form of the system of differential equations was eight dimensional in the two body problem and twelve dimensional in the three body problem. The convergence time for the relaxation method was at the order of seconds in both cases on a Pentium III.

8 Conclusion and Future Work

We presented a strategy for generating a family of smooth interpolating trajectories for a team of fully-actuated mobile robots. The family is parameterized by a scalar α. As α becomes closer to zero, the robots are pulled together as they move between the initial and final positions. The case $\alpha = 0.5$ corresponds to a totally uncoordinated strategy: each robot will move from its initial to its final position while minimizing its own energy. Finally, as α tends to 1, the robots try to preserve the distances between them and minimize the overall energy of the motion. This constitutes an alternative to generating motion for virtual structures by solving an optimization problem on the manifold of rigid body displacements $SE(3)$ [5].

While the paper provides a useful conceptual framework for optimal motion planning and generation of trajectories, there is a practical limitation to this work. As the number of robots, N increases, the generation of the Christoffel symbols and the solutions to the two-point boundary value problems become very complicated. Future work will be directed towards defining the necessary tools necessary to solve motion planning and control problems for large groups of robots. We believe that properly defined maps from the configuration space of the robots to smaller dimensional spaces capturing the behavior of the group will be central in this endeavour.

References

[1] Yamashita, A., Fukuchi, M., Ota, J., Arai, T., and Asama, H., 2000, "Motion Planning for Cooperative Transportation of a Large Object by Multiple Mobile Robots in a 3D Environment," *Proc. IEEE Int. Conf. Robot. Automat.*, San Francisco, CA, pp. 3144–3151.

[2] Kang, W., Xi, N., and Sparks, A., 2000, "Formation control of autonomous agents in 3D workspace," *Proc. IEEE Int. Conf. Robot. Automat.*, San Francisco, CA, pp. 1755–1760.

[3] Fox, D., Burgard, W., Kruppa, H., and Thrun, S., 2000, "Collaborative Multi-robot Exploration," Autonomous Robots, **8**(3), pp. 325–344.

[4] Balch, T., and Arkin, R. C., 1998, "Behavior-based Formation Control for Multi-Robot Teams," IEEE Trans. Rob. Autom., **14**(6), pp. 1–15.

[5] Parker, L. E., 2000, "Current State of the Art in Distributed Autonomous Mobile Robotics," *Proc. International Symposium on Distributed Autonomous Robotic Systems*, Knoxville, TN, pp. 3–12.

[6] L. Chaimowicz, Sugar, T., Kumar, V., and Campos, M., 2001, "An Architecture for Tightly Coupled Multi-robot Cooperation," *Proc. IEEE Int. Conf. Robot. Automat.*, Seoul, Korea, pp. 2992–2997.

[7] Spletzer, J., and Taylor, C. J., 2001, "A Framework for Sensor Planning and Control with Applications to Vision Guided Multi-Robot Systems," *Proc. IEEE Computer Society Conference on Computer Vision and Pattern Recognition*, Hawaii, USA.

[8] Chichka, D. F., Speyer, J. L., and Park, C. G., 1999, "Peak-seeking Control with Application to Formation Flight," *Proc. IEEE Conf. Decision and Control, Phoenix*, AZ, pp. 2463–2470.

[9] Fierro, R., Song, P., Das, A. K., and Kumar, V., 2002, "Cooperative Control of Robot Formations," *Cooperative Control and Optimization Series*, R. Murphey and P. Pardalos, eds., Kluwer Academic Press, pp. 73–93.

[10] Tan, K., and Lewis, M. A., 1997, "Virtual Structures for High-precision Cooperative Mobile Robot Control," Autonomous Robots, **4**(4), pp. 387–403.

[11] Beard, R. W., and Hadaegh, F. Y., 1998, "Constellation Templates: An Ap-

proach to Autonomous Formation Flying,'' *Proc. World Automation Congress*, Anchorage, Alaska.
[12] Zefran, M., Kumar, V., and Croke, C., 1995, ''On the Generation of Smooth Three-dimensional Rigid Body Motions,'' IEEE Trans. Rob. Autom., **14**(4), pp. 579–589.
[13] Bloch, A. M., Leonard, N. E., and Marsden, J. E., 2000, ''Controlled Lagrangians and the Stabilization of Mechanical Systems I: The First Matching Theorem,'' IEEE Trans. Autom. Control, **45**(12), pp. 2253–2270.
[14] Woolsey, C. A., Bloch, A. M., Leonard, N. E., and Marsden, J. E., 2001, ''Physical Dissipation and the Method of Controlled Lagrangians,'' *Proc. European Control Conference*, Porto, Portugal, pp. 2570–2575.
[15] Belta, C., and Kumar, V., 2002, ''An SVD-based Projection Method for Interpolation on $SE(3)$,'' IEEE Trans. Rob. Autom., **18**(3), pp. 334–345.
[16] Belta, C., and Kumar, V., 2001, ''Motion Generation for Formations of Robots: A Geometric Approach,'' *Proc. IEEE Int. Conf. Robot. Automat.*, Seoul, Korea.
[17] do Carmo, M. P., 1992, *Riemannian Geometry*, Birkhauser, Boston.
[18] Park, F. C., and Brockett, R. W. R. W., 1994, ''Kinematic Dexterity of Robotic Mechanisms,'' Int. J. Robot. Res., **13**(1), pp. 1–15.
[19] Belta, C., and Kumar, V., 2002, ''Euclidean Metrics for Motion Generation on $SE(3)$,'' J. Mech. Eng. Sci. Part C **216**(C1), pp. 47–61.
[20] Roth, B., 1981, ''Rigid and Flexible Frameworks,'' Am. Math. Monthly, **88**, pp. 6–21.
[21] Press, W. H., Teukolsky, S. A., Vetterling, W. T., and Flannery, B. P., 1998, *Numerical Recipes in C*, Cambridge University Press.